

Characterization of micrometer-size laser beam using a vibrating wire as a miniature scanner F SCI

Cite as: Rev. Sci. Instrum. **92**, 033303 (2021); <https://doi.org/10.1063/5.0028666>

Submitted: 09 September 2020 . Accepted: 25 January 2021 . Published Online: 03 March 2021

 S. G. Arutunian, A. V. Margaryan, G. S. Harutyunyan, E. G. Lazareva, A. T. Darpasyan,  D. S. Gyulamiryan,  M. Chung, and D. Kwak

COLLECTIONS

 This paper was selected as Featured

 This paper was selected as Scilight



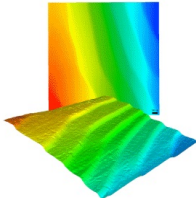
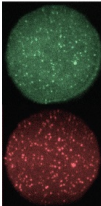
View Online



Export Citation



CrossMark

 <p>MAD CITY LABS INC. www.madcitylabs.com</p>	<p>Nanopositioning Systems</p> 	<p>Modular Motion Control</p> 	<p>AFM and NSOM Instruments</p> 	<p>Single Molecule Microscopes</p> 
---	--	--	---	--

Characterization of micrometer-size laser beam using a vibrating wire as a miniature scanner

Cite as: Rev. Sci. Instrum. 92, 033303 (2021); doi: 10.1063/5.0028666

Submitted: 9 September 2020 • Accepted: 25 January 2021 •

Published Online: 3 March 2021



View Online



Export Citation



CrossMark

S. G. Arutunian,^{1,a)}  A. V. Margaryan,¹ G. S. Harutyunyan,¹ E. G. Lazareva,¹ A. T. Darpasyan,²
D. S. Gyulamiryan,^{2,a)}  M. Chung,^{3,a)}  and D. Kwak³

AFFILIATIONS

¹Alikhanyan National Scientific Laboratory, 0036 Yerevan, Armenia

²Quantum College, 0046 Yerevan, Armenia

³Ulsan National Institute of Science and Technology, 44919 Ulsan, South Korea

^{a)}Authors to whom correspondence should be addressed: femto@yerphi.am; dav.gyulamiryan@gmail.com; and mchung@unist.ac.kr

ABSTRACT

A new method for profile measurements of small transverse size beams by means of a vibrating wire is presented. A vibrating wire resonator with a new magnetic system was developed and manufactured to ensure that the wire oscillated in a single plane. Presented evidence gives us confidence that the autogenerator creates vibrations at the natural frequency of the wire in a plane of the magnetic system, and these vibrations are sinusoidal. The system for measuring the laser beam reflected from the vibrating wire by means of a fast photodiode was upgraded. The experiments allowed the reconstruction of a fine structure of the focused beam of the semiconductor laser using only a few vibrating wire oscillations. The system presented here would eventually enable the implementation of tomographic measurements of the thin beam profile.

Published under license by AIP Publishing. <https://doi.org/10.1063/5.0028666>

I. INTRODUCTION

Micrometer-size beams of charged particles, radiation, and neutrons are of great interest in many areas of physics and technology.

Electron beams with extremely small transverse sizes and emittances are required for x-ray free-electron lasers (XFELs) and novel accelerator developments,¹ such as dielectric laser accelerators^{2–4} and plasma wakefield accelerators.^{5,6} In medicine and radiobiology, micrometer-size beams from charged particle accelerators or alpha sources have several distinct advantages.⁷ The use of micrometer or sub-micrometer beams results in lower doses of radiation and allows for targeted irradiation of damaged tissues. Optical biomedical imaging techniques (optical coherence tomography and Doppler optical coherence tomography) also deal with micrometer-size spots (from 250 μm down to 28 μm).⁸ Micrometer-size beams are also used in materials science and other areas of technology. For example, focused ion beam tomography is used for material fabrication and material in-service monitoring and deals with μm scale specimens⁹ and spacing in the range of 100 nm.¹⁰ For neutron optics, components such as micro-collimators, supermirrors, focusing monochromators, and specially designed neutron waveguides

have been developed to deliver neutron beams with cross sections in the sub-micrometer range.^{11,12}

Appropriate diagnostic and measurement methods are also needed when micrometer-size beams are used.

For two-dimensional profiling, techniques based on screens are usually used. The most direct method of observing beams is through the light emitted from a scintillation screen and detected by a CCD camera.^{13–16} Amorphous Si flat panel detectors and CMOS pixel detectors are also used. For neutron beams, Gd converters with the x-ray film and track etch foils with boron are adopted.¹⁷

Another widely used profiling method is scanning of a beam with a thin wire.^{16,18–20} Wire scanning is a unique diagnostic method whenever the beam characterization requires a high spatial resolution and, at the same time, a minimal interruption to the beam operation.²¹ There is also a class of profiling systems for measuring laser beams, which scans a beam profile with one or several pinholes, a slit, or a knife edge.^{22,23}

The idea of using the motion of a vibrating wire as a scanner has been suggested²⁴ (originally, a vibrating wire was used for the diagnostics of beams in accelerators based on the dependence of the frequency of oscillations of a wire on its temperature). The amplitude of vibrations of the developed resonators of the vibrating wire reaches

a few hundred micrometers.²⁴ Such a range of wire motion is well suited for profiling micrometer-size beams. The first experimental results described how profiling of the laser beam was performed and a criterion of reliability of the results was determined.²⁵ The experimental technique with laser beams has been further improved.²⁶ In the current study, we have continued in this direction by improving the magnetic resonator system of the vibrating wire and using more effective measuring systems.

II. PREVIOUS EXPERIMENTS AND BASIC UNITS OF THE NEW FACILITY

In the first experimental results on the use of a vibrating wire as a scanner for the profiling of micrometer-size beams, the laser beam of a semiconductor laser focused by a short-focus lens was measured.²⁵ The time of one measurement was 12.5 μ s. Profiling was performed for several hundred periods of wire oscillations. There was a large mismatch between forward and backward scans (we define forward scanning as the scanning when the wire moves in the positive direction of the transverse axis of coordinates), which, in this work, is explained by the inertia of the photodiode measuring system. The reconstruction of the profile is performed in one position of the vibrating wire. This experimental setup was subsequently improved.²⁶

The photodiode measurement electronics have been improved; in particular, capacitors have been removed from the photodiode load resistance circuit. The resonator with a vibrating wire was mounted on a bench with the feed orthogonal to the laser beam direction. The time per measurement, as in the previous experiment, was 12.5 μ s. A procedure was proposed to reconstruct the beam profile in absolute coordinates by means of several scans in different positions of the vibrating wire resonator relative to the transverse axis of the coordinates. Each scan in the beam profile formed a strip shape with a width of two amplitudes of the wire oscillations. If the offset between the strips is smaller than the width of the wire oscillation ranges, the two measured profiles have a common intersection area. By applying an overlapping procedure to the profiles measured in relative coordinates (the center of which coincides with the position of the resonator), the offset value can be determined in units of the amplitude of the wire oscillations. On the other hand, this offset is known in absolute coordinates by the resonator displacement, which is controlled by means of a micrometric feed. This feature allows normalization of the amplitude of wire oscillations in absolute coordinates. The profiles of two laser beams experimentally measured are observed in Refs. 25 and 26. The main criterion for the reliability of the results obtained here was the comparison of scanning in two different directions. Their mismatch was interpreted as an effect of the inertia of the measuring system, so it is important to choose a photodiode with a sufficient response. The measurement system of reflected photons plays an essential role. It has also been noted²⁶ that the mismatch between forward and reverse scanning can be associated with the unevenness of the wire motion (the center of the wire executes a figure-eight motion in a plane transverse to the wire). In this case, the central area of the wire, which plays the role of the scanner, goes through different parts of the beam when moving in opposite directions, and the results of the two opposite scans may not coincide. It is also important to select the proper position of the photodiode and its mounting system. In the current study, the basic

units of the experimental setup in our previous work²⁶ are updated, including the development and manufacture of a new magnetic system and the mounting unit of the photodiode. A new four-channel measurement board based on an analog-to-digital converter (ADC) with a 325 MHz full-power analog bandwidth was also developed. Instead of the previously used VBPW34S photodiode, a faster photodiode S1223-1 was installed. In addition, an RTB2004 oscilloscope with a sampling rate of 2.5 GSa/s (giga-samples per second) was used.

A. Vibrating wire resonator with a coupled magnetic system

It should be noted that the vibrating wire monitors were originally proposed for scanning the beams of charged particles using the dependence of the vibrating wire's frequency on heat deposition by beam particles scattered on the wire.²⁷ The performance criterion of the monitor was the stability of the wire's frequency, which, for time intervals of several hours, was ~ 0.01 Hz, with the value of the frequency itself in the range of several kHz.

In this work, we used a vibrating wire resonator with the following parameters: a wire length of 80 mm and a wire diameter of 100 μ m. Stainless steel was used as the wire material, which went through a special heat treatment (Germany standard 4401, hard). The use of such material increases the quality of the resonator, the tensile strength threshold, and frequency stability. Resonators of this type were often used in our experiments due to simplicity of assembly and the absence of frequency drift processes. In such resonators, the processes of autogeneration and stabilization of vibration amplitude are also easy to achieve. In terms of laser reflection, stainless steel is also a good material.

The frequency of the wire F is defined by the wire tension, which is set by the suspension system with a proper mass M attached $M = 4F^2L^2Sp/g$ (where L and S are the length and cross section of the wire, ρ is the wire material density, and g is the free-fall acceleration). For example, for a desired frequency of 1000 Hz, the mass of ~ 0.163 kg is needed. The following procedure is used: the direction of the wire is taken vertical, the upper clamp is pressed, and the lower clamp is released. Then, the required mass is suspended and the lower clamp is pressed. This procedure allows the desired frequency to be set to within ~ 10 Hz to 20 Hz.

The oscillations of the wire are generated by the interaction of an AC drive current through the wire with a permanent magnetic field and by a special autogeneration circuit (therefore, the wire material must be conductive). The vibrating wire is connected to a positive feedback circuit. The feedback source is the induced voltage on the wire, as it sweeps through the magnetic field. This voltage is amplified and is fed to the wire in the same phase. The process afterward is not entirely predictable and depends on the structure and strength of the magnetic field, tension, and mechanical properties of the wire and the quality of the wire pinch. In addition, the process depends on the values of the resistors in the feedback system. The excitation circuit also contains a non-linear element (junction field effect transistor) that stabilizes the amplitude of oscillation of the wire on which the process also strongly depends. The process of excitation of stable oscillations may contain a transition process in which the stable mode of oscillation occurs through the intermediate excitation of higher harmonics. All these

transitions are reflected in the signal directly measured from the wire.

The circuit consists of operational amplifiers with an external resistance on the order of a few 100 k Ω and amplifies the oscillation at a certain natural frequency. The amplitude of the drive current is stabilized by means of a junction field effect transistor (used as a voltage-controlled resistor) in a negative feedback loop on the level of a few mA.²⁸ The stabilization of the autogeneration drive current provides stabilization of mechanical oscillations of the wire.²⁴ The drive current depends on the feedback amplification factor and the level of the output signal, which is 2.2 V for sensors used in the experiments (wire voltage is ~ 40 mV, wire resistance is 8.3 Ω , and current through the wire is 4.8 mA). The amplitude of the wire's mechanical oscillation is determined by the current through the wire and the value of the magnetic field in the magnetic system gap, which is ~ 0.7 T to 0.8 T.²⁴ The vibrating wire has a very low drift related to the mechanical properties of the wire and resonator. A noise of about 0.01 Hz at a measuring interval of about 1 s is typical when using the vibrating wire resonator in the air. More significant are the slow variations caused by changes in ambient temperature. Of course, such variations are not essential for short time measurements of a few oscillation periods. The amplitude of the wire oscillations was measured using an optical microscope and was about two diameters of the wire. The method based on beam profiling in a few positions of the vibrating wire resonator allows us to determine the vibration amplitude more precisely (see Sec. VI A for details).

For the movement of the wire in the process of its own oscillations to be used as a scanning mechanism, the wire trajectory needs to be well defined in space. In our previous study, we assumed that the wire makes sinusoidal oscillations in one plane determined by the magnetic field in the gaps of the magnetic field system. The magnetic field for generating fluctuations of a wire at a natural frequency was created by a pair of magnetic poles with a console that fastens the wire on clamps. The size of the gap of the magnetic field was ~ 1 mm. The field in such gaps obviously has a certain barrel shape, and the planes of the separate poles may have a certain mismatch in the angle. To address these problems, a new magnetic system has been developed.

In our previous experiment,²⁶ we used a monitor in which the magnetic system consisted of two independent parts cantilevered on wire clamps with possible misalignment of the magnetic field planes. To ensure that the wire oscillations are flat, the system of separate magnetic poles was replaced by a new magnetic system consisting of two permanent neodymium–iron–boron magnets ($15 \times 10 \times 4$ mm³) with the same polarity to excite the first oscillation harmonic. These magnets were coupled with two polished strips of magnetic poles. An 8 mm diameter clearance was created at the center of the magnetic poles for the laser beam to pass through when being scanned by the vibrating wire. The length of the magnetic poles was 50 mm (with the length of the wire being 80 mm). In addition, the gap between the magnetic poles in which the wire vibrates was reduced from 1 mm to 0.6 mm. This improved the accuracy of parallelism of the magnetic poles over their entire length and reduced the effect of magnetic field non-uniformity in the gap. The new magnetic system is shown in Fig. 1(a). The optical scheme of the experiment is shown in Fig. 1(b).

The laser beam exits the monitor through the hole in the support [item 6 in Fig. 1(b)].

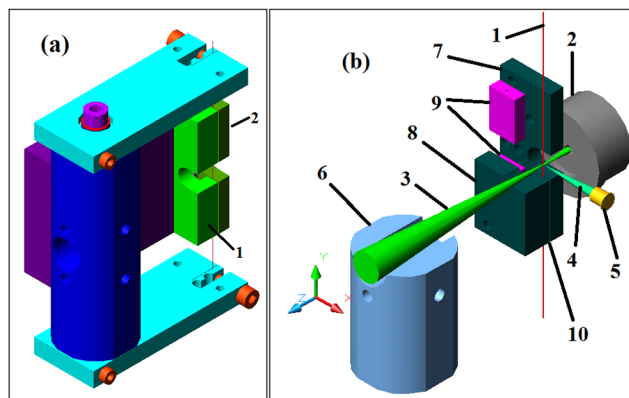


FIG. 1. Vibrating wire monitor resonators with a length of 80 mm: (a) A new magnetic system with coupled magnetic poles in the form of two polished plates (1 and 2). (b) Optical layout of the experiment: wire (1), lens (2), focused laser beam (3), reflected photons (4), photodiode (5), support (only the bottom half is shown) (6), first magnetic pole (7), second magnetic pole (only the bottom half is shown) (8), and permanent magnets (9). The magnetic field is confined between the magnetic poles in the horizontal direction, forming a magnetic field region of the order 0.7 T–0.8 T in the gap (10). Here, the coordinate system is also presented in which the wire is directed along the y-axis, oscillation of the wire occurs in the x direction, reflected photons are observed by a photodiode installed along the x-axis, and magnetic field and laser beam are aligned along the z-axis.

B. Laser, photodiode, photodiode measurement circuit, and photodiode mount system

In the scanning experiments, we used a diode-pumped solid-state laser JD-850 with a wavelength of 532 nm. The typical beam size of the laser beam was a few millimeters, so we used a lens with a 10 mm focal distance to achieve a sub-millimeter size.

Instead of the VBPW34S photodiode used in the previous study,²⁶ we used an S1223-1 photodiode (Hamamatsu) with a larger aperture and better response parameters. A comparison of the main characteristics of these photodiodes is shown in Table I.

In the experiment, the photons reflected by the vibrating wire were measured. In principle, it is best to perform this measurement

TABLE I. Comparison of the characteristics of fast photodiodes.

	VBPW34S	S1223-01
Radiant sensitive area (mm ²)	7.5	13
Terminal capacitance (pF)	40	20
	($V_R = 3$ V, $f = 1$ MHz)	
Cut-off frequency F_C (MHz)	3.5 ^a	20 (typical)
Dark current (nA)	2 ($V_R = 10$ V)	0.2
Noise equivalent power (W/Hz ^{1/2})	4×10^{-14} ($V_R = 20$ V)	1.4×10^{-14} ($V_R = 20$ V)

^a Calculated by rise time $t_R = 100$ ns (reverse voltage $V_R = 10$ V and load resistance $R_L = 1$ k Ω) by the formula $F_C = 0.35/t_R$ [Eqs. (3)–(5) in Ref. 29]. The conditions under which the given parameters were determined are given in brackets (f —characteristic frequency of the signal).

in a direction opposite to the laser beam propagation. In the previous experiment,²⁶ we tried to measure reflected photons as close as possible to this direction. For this purpose, the photodiode was mounted on a separate rod and introduced into the gap between the focusing lens and the vibrating wire. It has been noted, however, that this design is subject to vibrations and requires additional adjustment of the angle of the photodiode. In the new layout of the experiment, we decided to reduce the intensity of the reflected photons and to place the photodiode in the orthogonal direction to the laser beam propagation, thus eliminating the problem of photodiode vibration and greatly simplifying the alignment problem. According to studies on electromagnetic radiation diffraction on a cylinder in the orthogonal direction, significant radiation is also reflected (in terms of the angular distribution, the 90° scattering is 80% of the radiation scattering in the reverse direction).^{30,31}

The surface of the wire string used in the experiment is quite smooth, so the photodiode accepts mostly photons reflected at a certain angle from a narrow strip along the wire with a width much smaller than the diameter of the wire.

The entire wiring diagram is shown in Fig. 2. The circuit is based on the ATTINY2313 microcontroller.

To measure the photocurrent, we used the photodiode load resistance circuit (upper-left part in Fig. 2). The signal from the photodiode was amplified by the instrumentation amplifier (INA128) with excellent accuracy and controlled gain in the range from 1 to 10 000. The amplified signal from the instrumentation amplifier was fed to a fast ADC (AD9222) with the following parameters: 12-bit, signal-to-noise ratio = 70 dB (ratio = 10^7), and 325 MHz full-power analog bandwidth. We developed a fast operation mode when data from the ADC was immediately written to the block of 12 RAM (23LC512 with a memory of 512 kbit). Each output bit of the ADC was connected to one RAM in parallel. The process was executed by a serial peripheral interface (SPI). This type of synchronous serial communication interface is usually used for short-distance communication.

As the control of the recording process using microcontroller commands would slow down the process (a clock time of 62.5 ns for 16 MHz microcontroller quartz oscillator) and each command would consist of several cycles (at least two cycles for significant

commands), a control system using a 74HC00 medium integration logic chip with a 10 ns delay and an additional 10 MHz quartz oscillator was used. This logic provided a recording/reading process in the SPI mode directly between the ADC and the 10 MHz RAM without the microcontroller. By means of MC-LOG communication, only the start/stop recording was set by the microcontroller. In fact, one measurement was made every 100 ns. The maximum measurement stack time was 51.2 ms according to the RAM capacity. After the process was completed, the data were read out from the RAM and transferred to a PC via an RS232 interface at 2 Mbit/s.

The scheme also had a slow mode when the process of reading from the ADC using the same SPI protocol was performed by commands from the microprocessor. The maximum transmission speed in this case was limited by the MC-PC channel, and one measurement was made every 10 μ s. This mode allowed the use of the graphical capabilities of the computer and was often used in the process of configuring the experiment.

The signal from the photodiode after preamplification and other signals during the experiment were also measured with the RTB2004 oscilloscope, which allowed the simultaneous registration of several measurement channels. The main parameters of the RTB2004 are as follows: 300 MHz bandwidth, 4 analog/16 digital channels, maximum real time sampling rate of 2.5 GSa/s, memory depth per channel of 10 Msa, and segmented memory of 160 Mpoints.

III. EXPERIMENT LAYOUT

All units of the experiment were assembled on a heavy base of a measuring microscope (dimensions of $360 \times 450 \text{ mm}^2$), the moving bench of which had manual micrometric feeds with a stroke of 25 mm in two horizontal directions. The vibrating wire monitor with a photodiode was located on a movable bench. A laser with a beam alignment system and focusing lens was mounted on a fixed base. A photograph of the experimental setup is shown in Fig. 3.

A block diagram of the experiment is shown in Fig. 4. The RTB2004 oscilloscope was used to collect information from several

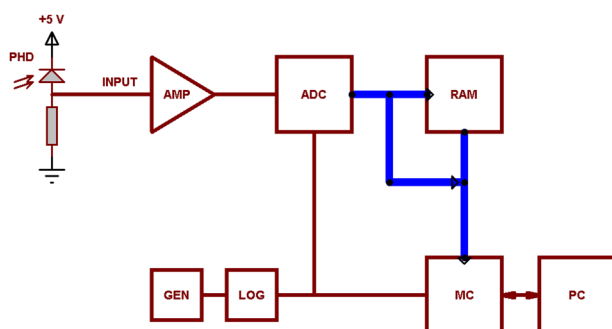


FIG. 2. Main units of the measurement scheme: photodiode (PHD), instrumentation amplifier (AMP), analog-to-digital converter (ADC), block of random access memory (RAM), quartz generator (GEN), logic block (LOG), microcontroller (MC), and computer (PC).

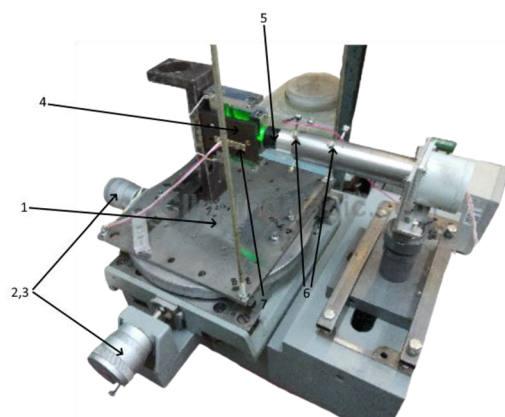


FIG. 3. Photograph of the experiment: mobile table (1) with micrometric feeds in two orthogonal directions (2 and 3), vibrating wire monitor (4), laser with focusing lens (5) and alignment system (6), and photodiode mounted on the base of the vibrating wire resonator (7).

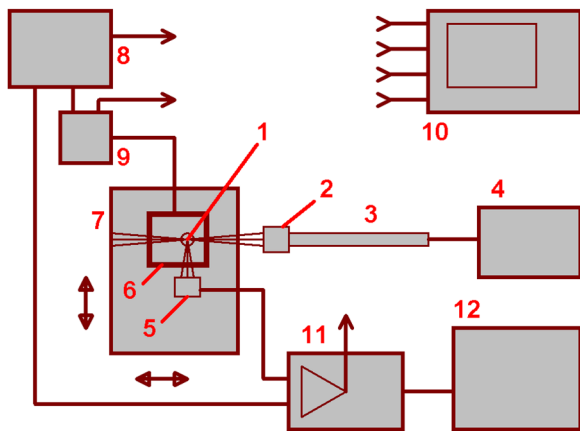


FIG. 4. Block diagram of the experiment: vibrating wire (1), focusing lens (2), laser (3) with a stabilized power supply unit (4), photodiode (5), resonator (6), movable bench (7), micrometric feed in two directions (marked by two-sided arrows), autogenerator of natural oscillations (8), controlled switch (9), the oscilloscope (10), measuring board (11), and computer (12).

channels in a timely manner. The photons reflected from the wire were registered by the photodiode. The wire was fixed to the resonator on which the photodiode was also mounted. The assembly of the monitor–photodiode was placed on the movable bench with micrometer feeds in two directions. The wires from the monitor were fed into the circuit of the autogenerator of natural oscillations through the controlled switch (the switch served as a trigger to start the oscilloscope measurements). The signal from the photodiode was recorded by a special measuring board. The primary amplifier unit outputs the signal to the oscilloscope.

The micrometric feed along the laser beam was used to position the wire in the vicinity of focal waist of laser beam. Orthogonal feed adjustments were used to enable the laser beam to scan the vibrating wire in several resonator positions.

IV. PRELIMINARY EXPERIMENTS

As noted above, the use of a vibrating wire as a scanner requires well-defined and stable vibrations of the wire in one plane in space. By “well-defined,” we mean that we know the position of the center of the vibrating wire in space as a function of time. In previous studies, it was assumed that such oscillations are sinusoidal and the center of the wire lies along a line (i.e., the oscillations of the wire take place in one plane).^{25,26} However, a question may arise as to whether the combination of the electronic excitation circuit and the resonator with the vibrating wire indeed excites the process of oscillations close to the free sinusoidal oscillations at the natural frequency. To answer this question, an experiment was carried out to sharply reset the excitation current through the wire irradiated by the focused laser beam. This was done together with simultaneous registration of the electrical signal from the wire (after the gain cascade) and the signal from the photodiode measuring the reflected photon flux. In this experiment, the profile of the laser beam served as a reference to study the oscillations of the wire after the autogeneration current was turned off. The current was

abruptly switched off with a special controlled switch (item 9 in Fig. 4).

Figure 5 shows the results of this experiment.

Since the electrical circuit equivalent to the vibrating wire resonator consists of a certain set of capacitors, inductors, and resistors,³² there can be a phase shift between the voltage signal directly on the wire and the output signal on autogeneration circuit. For the parameters of autogeneration circuit components used for this study, shift is small.

Figure 5 shows that the trigger signal caused a sharp break in the voltage signal stabilized by its amplitude from the wire (after ~ 1 ms, the autogenerator circuit started to excite a parasitic signal at the amplifier output). At the same time, the signal from the photodiode reflecting the real motion of the oscillating wire in the structured field of the laser beam did not undergo any changes. It is clear that even after an interruption of the excitation current through the wire, it continued to oscillate sinusoidally at its natural frequency. Since the type of oscillations measured by the photodiode had not changed, we can state that the autogeneration scheme we have developed excites sinusoidal oscillations of the wire at its natural frequency.

To confirm this, we also measured the electrical signal directly on the wire. The fact is that the voltage-controlled resistor used in the autogeneration circuit based on the junction field effect transistor has a significantly nonlinear voltage–ampere characteristic and can distort the signal spectrum. Figure 6(a) shows the signal measured on the wire. The shape of the signal on the wire is much closer to a sinusoidal one as compared to the shape of the amplified signal (yellow line in Fig. 5 until the auto-generation current shutdown). This is confirmed by the spectrum of the signal reconstructed with the oscilloscope. The Fourier-transformation of the signal from the wire [Fig. 6(b)] shows that the signal is practically sinusoidal and corresponds to one peak at the natural frequency of the wire oscillations. The amplitude of the signal on the wire is about 40 mV, whereas the emf formed as a result of the wire movement in the magnetic field is a significant value of about 12 mV (here, the



FIG. 5. Instantaneous shutdown of the autogeneration current through the wire. The time scale is $370 \mu\text{s}$ per division. Electrical signal at the output of the autogenerator circuit amplifier (yellow; see item 8 in Fig. 4), the trigger signal to switch off the current through the wire (green), and the signal from the photodiode (orange). Measurements were made with the multichannel oscilloscope RTB2004.

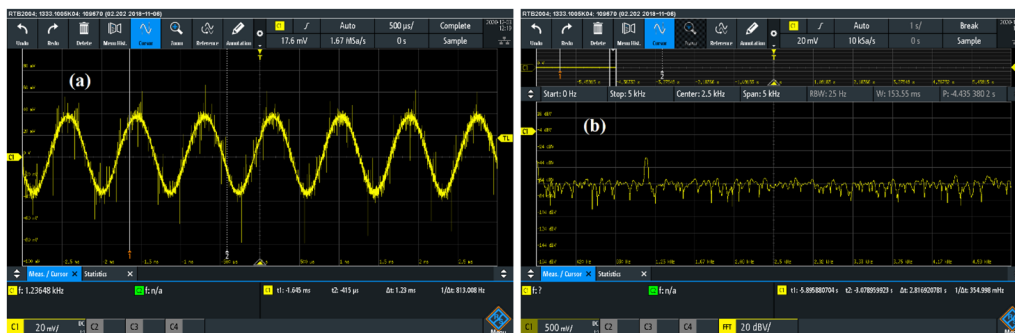


FIG. 6. Time dependence (a) and spectrum (b) of the signal immediately measured on the wire.

estimation was made for field in the magnetic system gaps of about 0.75 T, amplitude of the wire oscillations in the area of the magnet location about $130 \mu\text{m}$ with the total length of the magnetic field section of 30 mm, and frequency of the wire oscillations of about 1 kHz).

The experiment with an instantaneous shutdown of the auto-generation current also made it possible to estimate how fast the oscillation decay process takes place. It turned out that the signal decay takes place in about half a second and contains many hundreds of oscillation periods.

V. EXPERIMENTAL RESULTS

In this study, we measured the laser beam profile near the focus of the lens, which had a focal length of ~ 10 mm. This region was determined in advance by maximizing the number of photons reflected when the coordinate table moved along the z axis with a position correction along the x -axis [the coordinate system is defined in Fig. 1(b)].

The results of measurements with the RTB2004 oscilloscope at four monitor positions along the x -axis are shown in Fig. 7

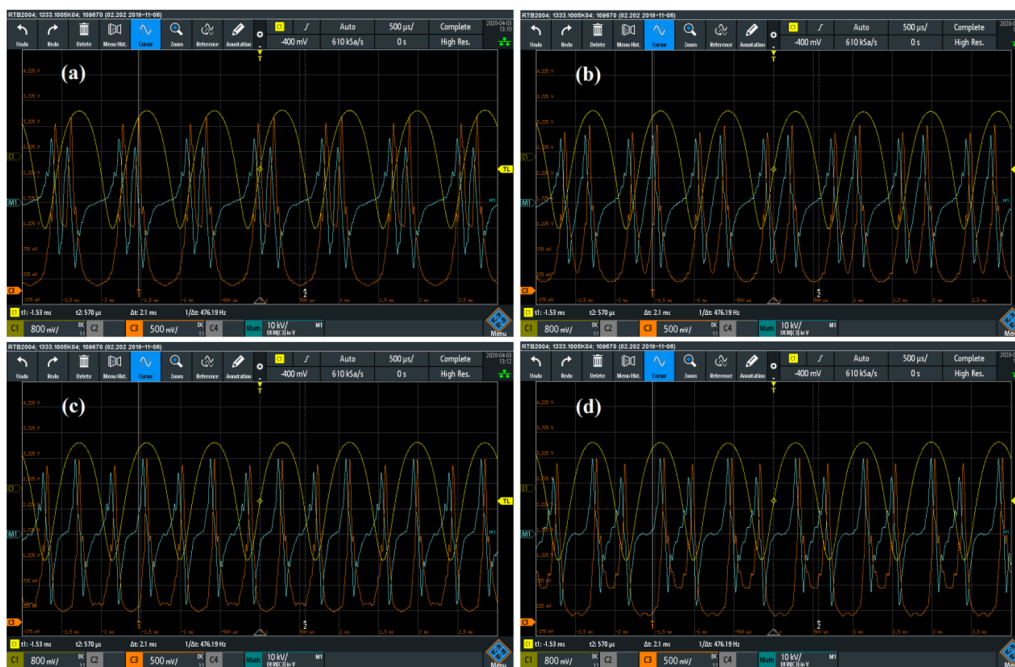


FIG. 7. Measurement of the electrical signals from the wire and from the output of the instrumentation amplifier of the photodiode measurement circuit and the derivative of the photodiode signal determined by an oscilloscope for four positions of the coordinate table in the x -axis direction: signal from the wire (yellow), signal from photodiode (orange), and derivative of the photodiode signal (blue). (a) 7.20 mm, (b) 7.15 mm, (c) 7.10 mm, and (d) 7.05 mm. It should be noted that in the case of (c), the point on the wire that reflects photons into the photodiode passes through the peak of the laser beam intensity as it crosses the midpoint of its oscillation (peaks in the photodiode response are equidistant, and the valleys in the orange curves are also symmetric).

(at 7.20 mm, 7.15 mm, 7.10 mm, and 7.05 mm). In addition to the electrical signal from the wire and the signal of reflected photons (after preamplification), Fig. 7 shows an oscillogram of the derivative of the photon signal obtained using a special mathematical function of the oscilloscope. There were approximately seven complete oscillations of the wire that were used to restore the profile of the laser beam.

Figure 7 shows good reproducibility of the fine structure of the photodiode signal from period to period. One period of signals from the wire and from the photodiode for the 7.15 mm position is shown in Fig. 8.

The extremes of the photodiode signal did not coincide with the extremes of the electrical signal from the wire, which, as noted above, were determined by the set of parameters of both the resonator and excitation circuit of natural oscillations. We considered the corresponding phase shift when restoring the laser beam profile, as described below. In addition, we observed a break in the symmetry in the photodiode signal relative to the extremes determined by the turning points of the wire direction. Considering the fact that the wire oscillations were flat and sinusoidal, as noted above, we concluded that similar to the previous studies,^{25,26} there was a delay effect in the dynamic response of the measuring system. Therefore, certain mathematical procedures were needed to reconstruct the beam profile.

VI. MATHEMATICAL PROCESSING AND EVALUATION OF MEASUREMENT ACCURACY

The mathematical processing of signals was conducted by matching each position of the wire in space with the number of reflected photons in that position. An electrical signal from the wire with a phase shift was used to determine the position of the wire in space. In addition, the inherent delay parameter of the measuring system needed to be considered. Time differentiation was used for this purpose as well as for the photodiode signal.



FIG. 8. One measuring period for the 7.15 mm position with a high resolution option of RTB2004: signal from the wire (yellow) and signal from the photodiode (orange). The measurements were made in the averaging mode with 2.5 (GSa/s), which in the high resolution option were averaged by the time period of 500 ns (corresponding to 2MSa/s).

A. Profile reconstruction

The real value of the reflected photons $f(t)$ was recovered by the output of the measurement system $g(t)$ after introducing the time constant of the system τ ²⁶ as

$$\tau \frac{dg(t)}{dt} + g(t) = f(t). \quad (1)$$

To calculate the center position of the wire in space, a sinusoidal model of movement was used in which the frequency was calculated from the average value of the oscillation period. For this purpose, we used the sinusoidal electric signal from the wire after its amplification by the operational amplifier without converting it into a rectangular signal, as done previously.^{25,26} What matters experimentally is that the autogeneration signal included a certain level of noise. The signal conversion was made based on the first part of the signal from the wire that intersected the set threshold. This led to uncertainty in the edge of the rectangular signal of the order of the level of signal noise.

The average period value was calculated as follows: We selected samples of points near the minima of the electric signal. Here, signals in the band $(-A_F, -0.75A_F)$ were considered, where A_F was the amplitude of the electric signal from the wire. Each of the samples was then regressed by a parabolic curve and a minimum point of this analytical function was chosen as a signal mark (see Fig. 9). The oscillation period T_F was calculated as the time difference of the consecutive marks.

The coordinates of the position of the wire center in space were calculated using the following formula:

$$x/A = \sin(2\pi t/T_F + \varphi), \quad (2)$$

where A is the amplitude of the wire oscillations (not yet defined) and φ is the phase shift between oscillations of the wire in space relative to the electric signal from the wire.

Because the RTB2004 oscilloscope provided a derivative of the measured signal, an attempt was made to reconstruct the beam profile from the photodiode signal using the instrumentation amplifier

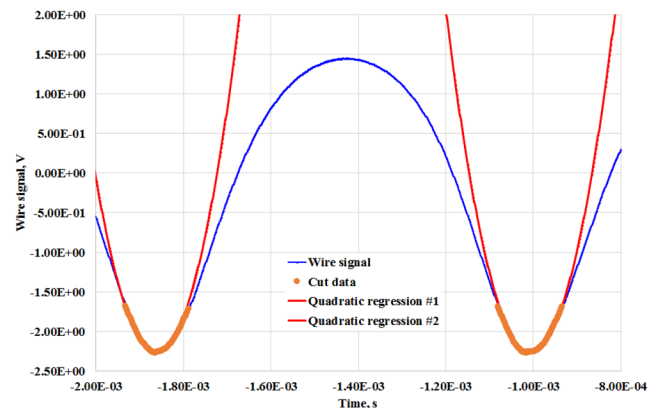


FIG. 9. Determination of oscillation periods by the minimum regression of the electric signal from the wire: signal from the wire (blue), samples of the signal from the wire in the area of minima (bold orange), and quadratic regression by the selected points (second-order polynomial fit, red).

and the corresponding derivative calculated by the oscilloscope. Fitting by undefined parameters τ and φ , however, did not lead to the expected result.

By “expected result,” we mean the alignment of the signal contours during forward and backward scanning. The results of such a fitting using some parameter τ values are shown in Fig. 10. For each value of τ , further scanning was performed by the parameter φ . The algorithm of coincidence of forward and reverse scanning gives a satisfactory result only at the tail of the distribution for $\tau = 10 \mu\text{s}$, where the photodiode signal derivative was small.

Instead of using the differential signal $dg(t)/dt$ from the oscilloscope, we calculated this function using the primary experimental dataset (t_i, P_i) from the photodiode as follows: for an arbitrary moving point, we selected $2n_0 + 1$ neighboring points $(i - n_0, i - n_0 + 1, \dots, i + n_0 - 1, i + n_0)$ on which linear regression was performed ($i = n_0, \dots, N - n_0$, where N is the number of experimental points). The regression coefficient a_i determining the slope of the linear approximation $P = a_i t + b_i$ is written as follows:

$$a_i = \frac{\sum t_j P_j - \sum t_j \sum P_j}{\sum t_j^2 - \sum t_j \sum t_j}, \quad (3)$$

where the index j is summed up over $(i - n_0, \dots, i + n_0)$. This value was taken as the value of the derivative at a given moving point. Note that the algorithm is similar to the known method of moving least squares estimation, which was used to estimate functions over a set of pointwise measurements (see Ref. 33).

The results of such an analysis for the set of measurements at the monitor position of 7.00 mm are shown in Fig. 11 for values $n_0 = 1, 2, 3$. Figure 11 also shows the signal differentiation from the photodiode using the oscilloscope.

Figure 11 shows that the differentiations of the photodiode signal using RTB2004 and calculated using the above algorithm were very different in areas with strong variations of the derivative. Therefore, the procedure of profile reconstruction was continued using the numerical differentiation of the primary signal from the photodiode for $n_0 = 3$. The results of fitting the parameters τ and φ for the three positions of the monitor of the laser beam profile are shown in

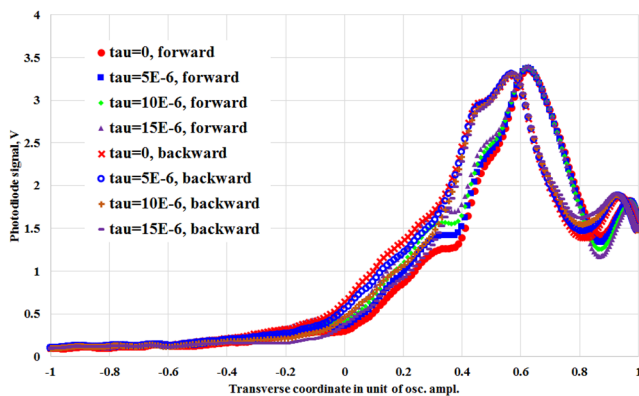


FIG. 10. Attempt to reconstruct the laser beam profile at the bench position of 7.00 mm using the RTB2004 differential signal for some values of $\tau = 0 \text{ s}$ (red), $\tau = 5 \mu\text{s}$ (brown), $\tau = 10 \mu\text{s}$ (green), and $\tau = 15 \mu\text{s}$ (blue).

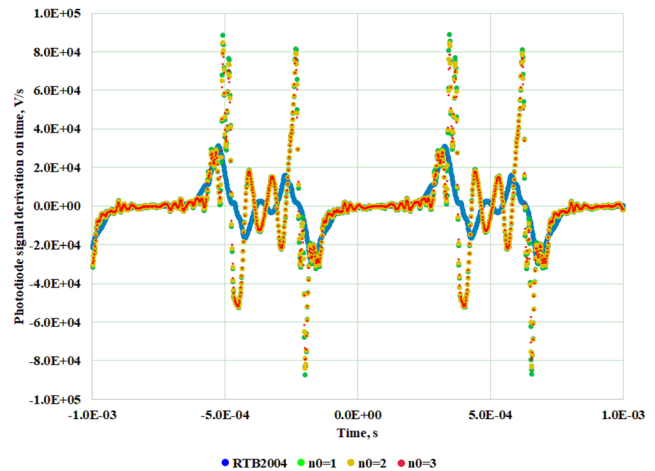


FIG. 11. Differentiation of the signal from the photodiode: with an oscilloscope (blue line), numerical differentiation of the primary signal for $n_0 = 1$ (gray points), $n_0 = 2$ (orange points), and $n_0 = 3$ (red points).

Fig. 12. In all three cases, we accepted $\varphi = 1.065$ and $\tau = 1.17 \times 10^{-5}$.

Scanning of the profile in several positions of the vibrating wire monitor allowed us to restore the profile of the beam in absolute coordinates. The method of determining the laser beam profile by superimposing the overlapping profiles in several resonator positions of the vibrating wire is similar to the creation of a panoramic image by the stitching procedure. Image stitching is the process that combines images with overlapped areas to form an image with a wide view. Usually, after inputting a series of images with overlapped areas, feature matching is applied to find the corresponding points of the images for stitching, and then, translation is done to align them properly.³⁴ It is important that this procedure allows us to separate the structure inherent to the profile (an analog of panorama) from that associated with the uncertainty of the wire movements (similar to camera defect).

For this purpose, as in the previous study,²⁶ profiles were shifted in coordinates relative to the center of the wire vibrations (here, at the position of 7.10 mm) to ensure the best features matching in overlapped areas of profiles. The magnitude of the shift was 0.335 in the amplitudes of the wire vibrations. Because the actual displacement of the monitor was $50 \mu\text{m}$, it was possible to reconstruct the beam profile in absolute coordinates [see Fig. 12(b)]. As 0.335 units in the amplitude of a wire oscillation correspond to $50 \mu\text{m}$, the amplitude of the wire oscillation is $149 \mu\text{m}$.

In addition, the beam profile was normalized to the maximum local density (corresponding to 3.755 V of the photodiode signal).

B. Evaluation of measurement accuracy

We estimated the accuracy of the profile measurement from the line width of the reconstructed profile, which included forward and backward scans. In the previous study,²⁶ this was done as follows: the profile was divided into nine overlapping strips, in each of which a set of reconstructed points was regressed using a quadratic polynomial. The mean error for all regressions was accepted as an error of the measured profile.

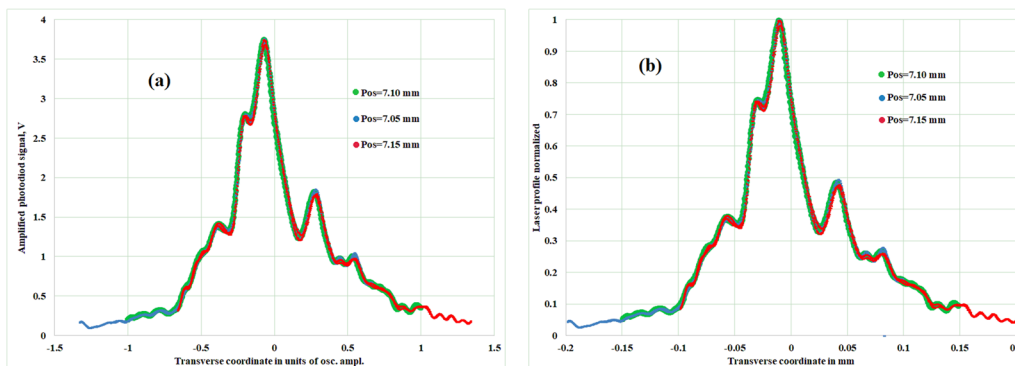


FIG. 12. The reconstruction of the laser beam profile using the numerical differentiation of the primary photodiode signal for $n_0 = 3$. (a) The transverse coordinate is represented in units of the amplitude of the wire oscillations relative to the oscillations center at 7.10 mm (green), 7.05 mm (blue), and 7.15 mm (red). The transverse shift (in amplitude units of the wire oscillation amplitude) has been applied to ensure the best matching with the 7.10 mm profile (in areas where these profiles overlap). (b) Reconstructing the laser beam profile in absolute coordinates: resonator position 7.10 mm (green), 7.05 mm (blue), and 7.15 mm (red).

The laser profile used in this experiment contained many fine details, so its approximation as a parabola in a wide range of transverse coordinates seems unsatisfactory. We proceeded in the same way as we numerically calculated the time derivative from the photodiode signal, where we used linear regression for a small set of neighboring points, and the linear regression coefficient was taken as the value of the derivative.

Because the profile was constructed from several passages of the wire across the laser beam, we used a set of points of the profile ordered by the coordinates. Then, we applied linear regression for the area of the selected point by the neighboring points, regardless of when these points were passed by the vibrating wire. Similarly, when calculating the time derivative, the number of neighbors was determined by the parameter n_0 (n_0 points with coordinates less than the selected one and n_0 points with coordinates greater than the selected one; thus, the total number of points was $2n_0 + 1$). By consistently applying this algorithm to all points of the reconstructed profile (except for the range edges), we calculated the mean squared errors Err (MSEs) of linear regression for several values of n_0 (see Fig. 13 for the results). Averaging the MSE over the entire scanning range was taken as a profile measurement error (see Fig. 13). Here is the summary of measurement errors: $n_0 = 1$ and $Err = 4.1 \times 10^{-6}$, $n_0 = 3$ and $Err = 1.9 \times 10^{-5}$, $n_0 = 5$ and $Err = 2.1 \times 10^{-5}$, and $n_0 = 7$ and $Err = 2.2 \times 10^{-5}$ [magnitude of the errors is expressed relative to the peak height (normalized to 1)].

As shown in Fig. 13, the error value was almost the same for values $n_0 = 3, 5,$ and 7 . When $n_0 = 1$, an unreliable result was produced because it resulted from a linear regression of only three points. Thus, we may consider the value for $n_0 = 5$, that is, $Err = 2.1 \times 10^{-5}$, as a standard error of the profile measurement. The corresponding average width of the profile line was \sqrt{Err} (square root of MSE). This is the value to be used when estimating the noise level in the signal-to-noise ratio, which is 224.³⁵

To evaluate the divergence of forward and backward scans, we have also proposed a fast algorithm, which consisted of integrating the reconstructed profile from the photodiode along the transverse coordinate of the center of the wire for one period. When the direction of the wire changed, the integration sign changed so that for

matched forward and backward scans, these integrals shrank. For real profiles, the procedure defines the area enclosed between the forward and reverse scan lines. The smaller the mismatch value, the smaller the integrals. Note, however, that this criterion cannot serve as a basis for parameter fitting of τ and φ because this area represents an integral of the alternating function from the coordinate and may be small, despite the large differences between the forward and reverse scans. Nevertheless, for quick estimation of an already calibrated scanning system, including the photodiode and its measurement system, this algorithm may be of interest for operational control of the scanning process.

Figure 14 shows an example of the implementation of such an algorithm for one of the scanning periods at the vibrating wire resonator at the position of 7.10 mm. The integral of the forward scanning profile in Fig. 14(a) gives a value of 0.625 83, while the integral

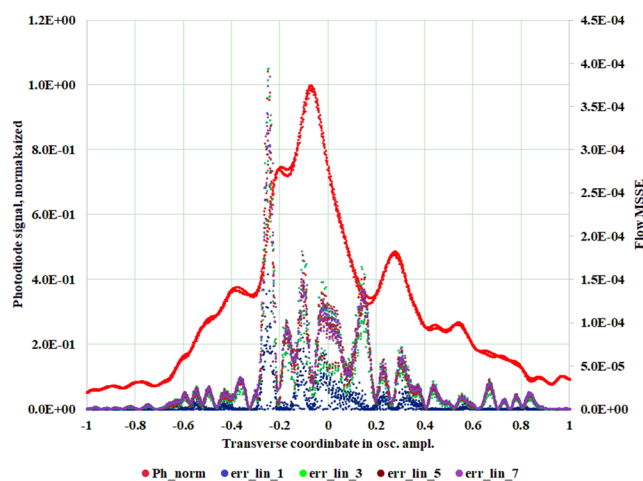


FIG. 13. A reconstructed laser beam profile normalized to the maximum local density (transverse coordinate in units of the amplitude of the wire oscillations, red). Also shown are errors for different values of the parameter n_0 : 1 (dark blue), 3 (green), 5 (dark-red), and 7 (magenta).

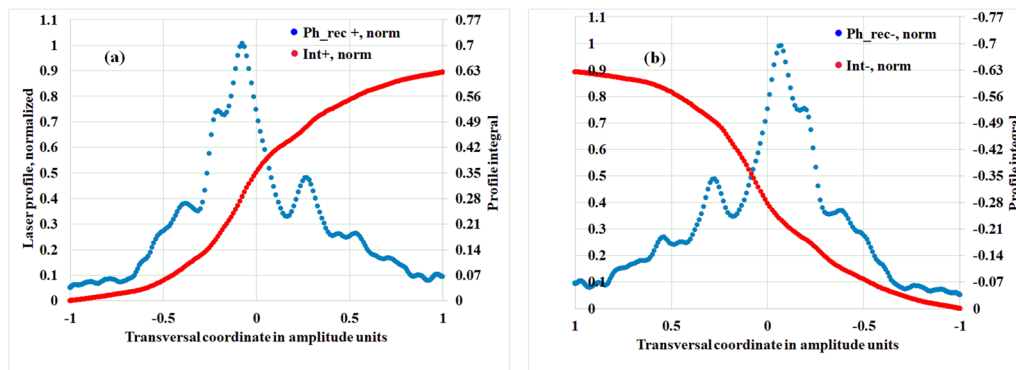


FIG. 14. Forward (a) and backward (b) scan profiles for one period of wire oscillation. In (a), transversal coordinates are presented in ascending order (from -1 to 1), and the reconstructed profile for the first half-period (blue) and corresponding integral over transversal coordinate (red) are plotted. In (b), transversal coordinates are presented in descending order (from 1 to -1), and the reconstructed profile for second half-period (blue) and continuation of the integral (from $+1$ to -1 , red) are plotted.

of the reverse scanning profile in Fig. 14(b) gives a value of -0.625 14. The sum of these values 0.0007 defines a discrepancy between the profiles.

VII. CONCLUSION

Upgrades of the experimental layout, namely, a new magnetic field system providing better magnetic field flatness, the use of a photodiode with better parameters, a new measurement system based on a precision instrumentation amplifier and fast analog-to-digital converter, and an oscilloscope RTB2004, have significantly improved the profile resolution and revealed many detailed and well-reproducible features of the focused laser beam. The accuracy of the measurements was significantly improved, and the measurement time was reduced.

As mentioned above, when measuring laser beams, the photodiode collects photons reflected by a narrow strip along the wire (the surface of the stainless steel wire is quite smooth). In this regard, tungsten wires with a gold coating can be promising. Such wires have excellent mechanical characteristics, and the gold layer would provide a good reflectivity.

For measuring beams of charged particles or neutrons, instead of surface reflection, scattering processes in the volume of the wire will be important. In addition, to obtain the required resolution, a thinner wire should be used. We have an experience in fabricating resonators with wires up to $20\ \mu\text{m}$ in diameter. Composite wires containing thin markers (e.g., a thin core or a narrow strip with another material sprayed on the surface of the wire) can also be used. Flat wires oriented with their narrow side along the beam, etc., may be of interest.

Instrumental factors of the present method should also be further investigated for the future research. The main issue here is the precise information on the wire motion. In this work, a model of sinusoidal motion of the wire was used, which gave consistent results of the profile at forward and backward scans. Profile recovery by measurements in a number of positions along the transverse coordinate was also quite effective.

We plan to further improve the measurement system in order to obtain information about the profile without the need to correct

the data with respect to the system delay. This will make it possible to measure the beam profile in one oscillation of the vibrating wire, that is, in less than $1\ \text{ms}$. With fewer fitting parameters related to the measurement system delay, it will be easier to catch the effects of higher harmonics in the wire motion. Finally, an important criterion will be to compare the results with alternative CCD camera-based profile measurements.

A practical solution to these problems will allow the approach of micrometer-size beam tomography, that is, determining the two-dimensional profile of the beam by a set of one-dimensional profiles.

ACKNOWLEDGMENTS

This work was supported by the RA MES SCS in the framework of Project No. 18T-1C031.

This work was also supported by the National Research Foundation (NRF) of Korea (Grant No. NRF-2020R1A2C1010835) and Pohang Accelerator Laboratory (Project No. 2.200892.01).

DATA AVAILABILITY

The data that support the findings of this study are available from the corresponding authors upon reasonable request.

REFERENCES

- ¹S. Borrelli, G. L. Orlandi, M. Bednarzik, C. David, E. Ferrari, V. A. Guzenko, C. Ozkan-Loch, E. Prat, and R. Ischebeck, "Generation and measurement of sub-micrometer relativistic electron beams," *Commun. Phys.* **1**, 52 (2018).
- ²R. J. England, R. J. Noble, K. Bane, D. H. Dowell, C.-K. Ng, J. E. Spencer, S. Tantawi, Z. Wu, R. L. Byer, E. Peralta, K. Soong, C.-M. Chang, B. Montazeri, S. J. Wolf, B. Cowan, J. Dawson, W. Gai, P. Hommelhoff, Y.-C. Huang, C. Jing, C. McGuinness, R. B. Palmer, B. Naranjo, J. Rosenzweig, G. Travish, A. Mizrahi, L. Schachter, C. Sears, G. R. Werner, and R. B. Yoder, "Dielectric laser accelerators," *Rev. Mod. Phys.* **86**, 1337–1389 (2014).
- ³M. I. Ivanyan, L. V. Aslyan, K. Floettmann, F. Lemery, and V. M. Tsakanov, "Wakefields in conducting waveguides with a lossy dielectric channel," *Phys. Rev. Accel. Beams* **23**, 041301 (2020).
- ⁴A. D. Kanareykin, "Low loss microwave ceramic and other microwave dielectric materials for beam physics applications," *J. Russ. Univ. Radioelectron.* **22**(4), 66–74 (2019).

- ⁵E. Brunetti, R. P. Shanks, G. G. Manahan, M. R. Islam, B. Ersfeld, M. P. Anania, S. Cipiccia, R. C. Issac, G. Raj, G. Vieux, G. H. Welsh, S. M. Wiggins, and D. A. Jaroszynski, "Low emittance, high brilliance relativistic electron beams from a laser-plasma accelerator," *Phys. Rev. Lett.* **105**, 215007 (2010).
- ⁶M. C. Downer, R. Zgadzaj, A. Debus, U. Schramm, and M. C. Kaluza, "Diagnostics for plasma-based electron accelerators," *Rev. Mod. Phys.* **90**, 035002-1–035002-62 (2018).
- ⁷S. Gerardi, "A comparative review of charged particle microbeam facilities," *Radiat. Prot. Dosim.* **122**(1-4), 285–291 (2006).
- ⁸Y. Mao, S. Chang, S. Sherif, and C. Fluerau, "Fiber lenses for ultra-small probes used in optical coherent tomography," in *Proceedings of the 6th International Conference on Photonics and Imaging in Biology and Medicine (PIBM 2007), Wuhan, China, November 2007* (World Scientific, Singapore, 2008), pp. 228–237.
- ⁹G. Moebus and B. J. Inkson, "Nanoscale tomography in materials science," *Mater. Today* **10**(12), 18–25 (2007).
- ¹⁰L. Holzer, B. Muench, M. Wegmann, P. Gasser, and R. J. Flatt, "FIB-nanotomography of particulate systems—Part I: Particle shape and topology of interfaces," *J. Am. Ceram. Soc.* **89**(8), 2577–2585 (2006).
- ¹¹N. W. Parker, A. D. Brodie, and J. H. McCoy, "A high throughput NGL electron beam direct-write lithography system," *Proc. SPIE* **3997**, 713–720 (2000).
- ¹²F. Pfeiffer, V. Leiner, P. Hoeghoej, and I. Anderson, "Submicrometer coherent neutron beam production using a thin-film waveguide," *Phys. Rev. Lett.* **88**(5), 055507 (2002).
- ¹³P. Forck, *Lecture Notes on Beam Instrumentation and Diagnostics* (Gesellschaft für Schwerionenforschung (GSI), Joint University Accelerator School, Darmstadt, Germany, 2011), p. 143.
- ¹⁴R. Jung, G. Ferioli, and S. Hutchins, "Single pass optical profile monitoring," in *Proceedings of the DIPAC 2003, Mainz, Germany, May 2003*, <http://www.jacow.org>, pp. 10–14.
- ¹⁵P. Forck, C. A. Andre, F. Becker, R. Haseitl, A. Reiter, B. Walasek-Höhne, W. Ensinger, and K. Renuka, "Scintillation screen investigations for high energy heavy ion beams at GSI," in *Proceedings of the DIPAC 2011, Hamburg, Germany, May 2011*, <http://www.jacow.org>, pp. 170–173.
- ¹⁶G. Kube, "Particle beam diagnostics and control," in *Laser-Plasma Acceleration: Proceedings of the International School of Physics "Enrico Fermi", Varenna on Lake, 20–25 June 2011*, edited by F. Ferroni and L. A. Gizzi (IOS Press, Societa Italiana di Fisica, 2012), p. 102.
- ¹⁷Neutron imaging at the spallation source SINQ. Information for potential users and customers, Broschuere Neutron Imaging_Nutzer_e, 09.2011; 20_Neutron_Imaging_m3 (PSI).pdf.
- ¹⁸P. Strehl, *Beam Instrumentation and Diagnostics* (Springer-Verlag, Berlin, Heidelberg, 2006).
- ¹⁹K. Wittenburg, "Beam halo and bunch purity monitoring," [arXiv:2005.07027](https://arxiv.org/abs/2005.07027) (2005).
- ²⁰D. M. Harryman and C. C. Wilcox, "An upgraded scanning wire beam profile monitoring system for the ISIS high energy drift space," in *Proceedings of IBIC 2017, Grand Rapids, MI, USA, August 2017*, <http://www.jacow.org>, pp. 396–400.
- ²¹G. L. Orlandi, P. Heimgartner, R. Ischebeck, C. Ozkan Loch, S. Trovati, P. Valitutti, V. Schlott, M. Ferianis, and G. Penco, "Design and experimental tests of free electron laser wire scanners," *Phys. Rev. Accel. Beams* **19**, 092802 (2016).
- ²²See <https://www.rp-photonics.com/beamprofilers.html> for scanning beam profilers based on slits, knife edges, or pinholes.
- ²³M. Sheikh and N. A. Riza, "Demonstration of pinhole laser beam profiling using a digital micromirror device," *IEEE Photonics Technol. Lett.* **21**(10), 666–668 (2009).
- ²⁴S. G. Arutunian, M. Chung, G. S. Harutyunyan, A. V. Margaryan, E. G. Lazareva, L. M. Lazarev, and L. A. Shahinyan, "Fast resonant target vibrating wire scanner for photon beam," *Rev. Sci. Instrum.* **87**, 023108 (2016).
- ²⁵E. G. Lazareva, "Vibrating wire for profile measurements of thin beams in particle accelerators: Preliminary tests using a laser beam," *J. Contemp. Phys. (Arm. Acad. Sci.)* **53**(2), 136–145 (2018).
- ²⁶S. G. Arutunian, S. A. Badalyan, M. Chung, E. G. Lazareva, A. V. Margaryan, and G. S. Harutyunyan, "A method for profile measurements of small transverse size beams by means of a vibrating wire," *Rev. Sci. Instrum.* **90**, 073302 (2019).
- ²⁷S. G. Arutunian, M. R. Mailian, and K. Wittenburg, "Vibrating wires for beam diagnostics," *Nucl. Instrum. Methods Phys. Res., Sect. A* **572**, 1022–1032 (2007).
- ²⁸S. G. Arutunian, A. E. Avetisyan, M. M. Davtyan, G. S. Harutyunyan, I. E. Vasiniuk, M. Chung, and V. Scarpine, "Large aperture vibrating wire monitor with two mechanically coupled wires for beam halo measurements," *Phys. Rev. Spec. Top.—Accel. Beams* **17**, 032802-1–032802-11 (2014).
- ²⁹See https://www.hamamatsu.com/resources/pdf/ssd/e02_handbook_si_photo_diode.pdf for photodiode rise time calculations.
- ³⁰A. I. Potekhin, *Nekotorie Zadachi Difrakcii Elektromagnitnikh Voln* (Sovetskoe Radio, Moskva, 1948) (in Russian).
- ³¹L. D. Goldshteyn and N. V. Zernov, *Elktromagnitnie Polya I Volni* (Sovetskoe Radio, Moskva, 1971) (in Russian).
- ³²A. A. H. Pádua, J. M. N. A. Fareira, J. C. G. Calado, and W. A. Wakeham, "Electromechanical model for vibrating-wire instruments," *Rev. Sci. Instrum.* **69**, 2392–2399 (1998).
- ³³R. V. Garimella, "A simple introduction to moving least squares and local regression estimation," Los Alamos National Laboratory, Report No. LA-UR-17-24975, USA, 20 June 2017.
- ³⁴Z. Wang and Z. Yang, "Review on image-stitching techniques," *Multimedia Syst.* **26**, 413 (2020).
- ³⁵Note that the calculated value of the standard square error of measurement $= 2.08 \times 10^{-5}$ is more than an order of magnitude smaller than the similar value 3.25×10^{-4} , calculated in Ref. 26 (the corresponding width of the profile line was 0.018 units of the maximum local density).